

2008

Analysis of Expansion Waves Appearing in the Outlets of Two-Phase Flow Nozzles

Masafumi Nakagawa
Toyohashi University of Technology

Atsushi Harada
Toyohashi University of Technology

Menandro Serrano Berana
Toyohashi University of Technology

Follow this and additional works at: <http://docs.lib.purdue.edu/iracc>

Nakagawa, Masafumi; Harada, Atsushi; and Berana, Menandro Serrano, "Analysis of Expansion Waves Appearing in the Outlets of Two-Phase Flow Nozzles" (2008). *International Refrigeration and Air Conditioning Conference*. Paper 925.
<http://docs.lib.purdue.edu/iracc/925>

This document has been made available through Purdue e-Pubs, a service of the Purdue University Libraries. Please contact epubs@purdue.edu for additional information.

Complete proceedings may be acquired in print and on CD-ROM directly from the Ray W. Herrick Laboratories at <https://engineering.purdue.edu/Herrick/Events/orderlit.html>

Analysis of Expansion Waves Appearing in the Outlets of Two-Phase Flow Nozzles

Masafumi NAKAGAWA¹, Atsushi HARADA¹, Menandro Serrano BERANA^{1,2,*}

¹Toyohashi University of Technology, Department of Mechanical and
Structural System Engineering, Toyohashi City, Aichi, Japan;
Tel.: +81 (53) 244-6670, Fax: +81 (53) 244-6661, Email: berana@nak.mech.tut.ac.jp

²University of the Philippines-Diliman, Department of Mechanical
Engineering, Quezon City, Metro Manila, Philippines;
Tel./Fax: +63 (2) 920-8875, Email: msberana@up.edu.ph (on study leave)

* Corresponding Author

ABSTRACT

Two-phase flow nozzles are used in the total flow systems of geothermal power plants and in the ejector-refrigeration cycle. The purpose of the present study is to theoretically elucidate the characteristics of expansion waves at the outlets of supersonic two-phase-flow nozzles. Two-dimensional basic equations for compressible two-phase flow were derived by incorporating the equation of inter-phase momentum transfer into equations of gas dynamics. In this study, the theoretical analyses were carried out by focusing on momentum-relaxation phenomena in high-speed mist flow. Expansion waves occurring right after two-phase flow nozzles were calculated by using the CIP method. The calculated expansion curves were compared with the experimentally obtained ones. The shape of the calculated ones closely resembled the shape of the experimentally obtained ones.

1. INTRODUCTION

Two-phase nozzles are used in total-flow systems of geothermal power plants (Mori and Suyama, 1980) and in the ejector of ejector refrigeration systems (Nakagawa, 2004). One of the most important functions of the nozzles is to convert thermal energy into kinetic energy. The kinetic energy of the two-phase flow exhausted from nozzles is used to rotate turbine wheels in geothermal power plants and to compress the suctioned vapor in the ejectors of ejector-refrigeration systems. The sound speeds in those nozzles are usually very low (Landau and Lifshitz, 1959), so the two-phase flows in those nozzles have to be accelerated into supersonic state. The energy conversion efficiency of the nozzles is too low because of the transport problems peculiar to two-phase flow. So, we studied several ways on how to improve the energy conversion efficiency of the nozzles (Nakagawa *et al.*, 1998).

When the kinetic energy of the two-phase flow flushing out from a nozzle is used, it is necessary to control the occurrence of shock waves and expansion waves. It is also necessary to design a nozzle which can work at any state. In particular, it is important to elucidate the mixing process of the two-phase flow and the suctioned vapor in the mixing section of the two-phase ejector in an ejector refrigeration cycle. There are many studies (Nakagawa and Mamiya, 1998) that treat the expansion wave of two-phase flow with phase change in one-dimensional approach. However, there are only few that treat it in two-dimensional approach (Marble, 1963).

The expansion waves of steam flow at a nozzle outlet (Nakagawa *et al.*, 2007) were experimentally verified in this research.

This study focuses on the momentum-relaxation phenomena between the phases of high-speed mist flow. The objective of this study is to elucidate the theoretical characteristics of the expansion waves at the outlet of a supersonic two-phase flow nozzle.

2. THE BASIC EQUATIONS

The momentum relaxation phenomena are very important in high speed two-phase flow. In this paper, phase change was neglected but the compressibility of the gas was considered for simplicity. The continuity equations of the gas and the liquid phases were expressed as

$$\frac{\partial}{\partial t} \alpha \rho_g + \frac{\partial}{\partial x_j} \alpha \rho_g v_{gj} = 0, \quad (1)$$

$$\frac{\partial}{\partial t} (1-\alpha) \rho_l + \frac{\partial}{\partial x_j} (1-\alpha) \rho_l v_{lj} = 0. \quad (2)$$

Where, ρ is density, v is velocity, and α is void fraction which is the volume fraction of the gas phase, t is time and x_j is assigned as a coordinate axis. Subscripts g and l indicate gas and liquid phases, respectively.

The momentum equations were expressed as follows:

$$\alpha \rho_g \frac{\partial v_{gi}}{\partial t} + \alpha \rho_g v_{gj} \frac{\partial v_{gi}}{\partial x_j} = -(1-\alpha) \rho_l \frac{v_{gi} - v_{li}}{\tau} - \alpha \frac{\partial p}{\partial x_i}, \quad (i = 1, 2), \quad (3)$$

$$(1-\alpha) \rho_l \frac{\partial v_{li}}{\partial t} + (1-\alpha) \rho_l v_{lj} \frac{\partial v_{li}}{\partial x_j} = (1-\alpha) \rho_l \frac{v_{gi} - v_{li}}{\tau} - (1-\alpha) \frac{\partial p}{\partial x_i}, \quad (i = 1, 2). \quad (4)$$

Where, p is pressure, τ is relaxation time expressed as $\rho d^2 / 18 \mu_g$, d is diameter of the droplets and μ_g is the coefficient of viscosity of the gas.

In this study, the quality x of the two phase flow was given a value of 0.1. If the droplet was very small in this condition, Stokes frictional drag was considered to act on the droplet. As a result, the drag force was written as external force per unit volume in equations (3) and (4). The gas phase was assumed to be a perfect gas and assumed to be changing isothermally because the heat capacity of the liquid was very big. The compressibility of the liquid was very much smaller than that of the gas, so the liquid droplets were assumed to be incompressible. It was assumed that the droplets were not colliding and not aggregating with each other and not breaking up. Droplets diameter was assumed to be constant.

The state equation of each phase was written as

$$\frac{p}{\rho_g} = const., \quad (5)$$

$$\rho_l = const.. \quad (6)$$

In equations (3) and (4), the velocity difference between the gas and the liquid phase is becoming small as a result of large exchange of momentum when τ is small. If τ is 0, equilibrium in velocity of the flow is established. The vapor and droplets have the same velocity in this case. At larger τ , the momentum exchange between the phases is negligible. If τ is infinity, frozen flow is established. There is no interaction between the phases. The vapor and the droplets flow independently from each other.

The differential terms of equations (1)-(4), which control the momentum-relaxation phenomena of two-phase flow, were the same as the basic equations of frozen flow. The dimensionless parameters of the equations were controlled by the Mach number of the frozen flow.

3. SOUND SPEED

Sound speed is defined as the propagation speed of disturbance in static fluid. The propagation speed of the microscopic disturbance in two-phase flow was obtained from linearization of equations (1)-(6). If the microscopic

disturbance was transmitted at a frequency ω , complex propagation number $\mathbf{k} = (k_x, k_y)$ would be obtained from the linear equations. Then, the square of the sound speed a^2 was obtained.

$$a^2 = \frac{\omega^2}{k_x^2 + k_y^2} = \frac{i \left(\frac{p}{\rho_l} \right) \left\{ (1-\alpha)\rho_g + \alpha\rho_l \right\} \omega\tau - \left(\frac{p}{\alpha} \right)}{i\alpha\rho_g\omega\tau - \left\{ \alpha\rho_g + (1-\alpha)\rho_l \right\}}. \quad (7)$$

When τ is 0 in equation (7), the sound speed of the equilibrium flow is obtained as

$$a_e = \sqrt{\frac{p}{\alpha(\alpha\rho_g + (1-\alpha)\rho_l)}}. \quad (8)$$

Where, the subscript e denotes equilibrium condition.

If τ is infinity, the sound speed of the frozen flow is calculated as

$$a_f = \sqrt{\frac{p}{\rho_g} + \frac{p(1-\alpha)}{\rho_l}}. \quad (9)$$

Where, the subscript f denotes frozen condition. If $\rho_l \gg \rho_g$, the frozen sound speed is approximately equal to the isothermal sound speed of the gas. Therefore, a sound speed that is non-dimensionalized by the isothermal sound speed of the gas $a' = a/(p/\rho_g)^{1/2}$ approaches unity.

The propagation speed or sound speed calculated using equation (7) at x of 0.1 and density ratio ρ_l/ρ_g of 10^3 was plotted in Figure 1. Those chosen values of physical properties were taken from the steam data. The vertical and the horizontal axes of Figure 1 are the non-dimensional sound speed a' and $\omega\tau$, respectively. When $\omega\tau$ was smaller than 1, the sound was nearly equal to the equilibrium sound speed. Conversely, when $\omega\tau$ is larger than 20, the sound speed is approximately equal to the frozen sound speed.

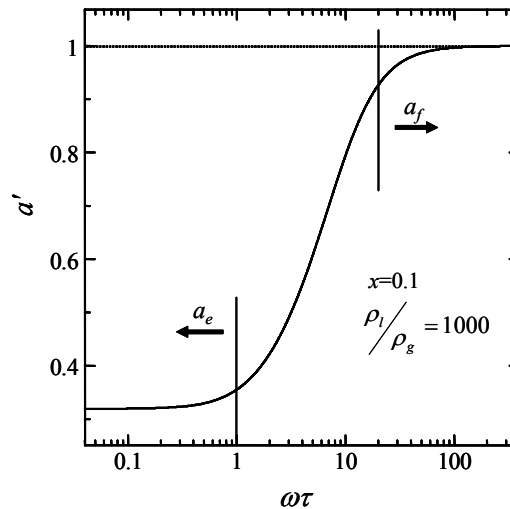


Figure 1: Sound velocity of two-phase flow with momentum relaxation

4. ANALYTICAL MODEL

In analyzing the expansion wave at the nozzle outlet, the analysis has to be carried out starting in the nozzle, to the nozzle outlet and then after the nozzle. The two-phase flow in the nozzle was assumed to be fully developed so the pressure gradient was taken as constant. Then, the inlet condition of the nozzle was determined through those conditions.

Fig.2 shows the flow field that we used in analytical modeling. The analytical area was divided into the diverging section of the nozzle and the back-pressure chamber. The boundary condition at the top was set to symmetric condition because it was the center axis of the nozzle. The lower and the right parts were set as free outlets.

The inlet condition of the nozzle was determined by using the basic equations of one-dimensional two-phase flow which were obtained from equations (1)-(4). The difference in velocities between the gas and the liquid were expressed as

$$v_g - v_l = \left(\frac{\alpha}{1-\alpha} \frac{\tau}{\rho_l} - \frac{\alpha}{1-\alpha} \frac{\rho_g}{\rho_l} \frac{\tau}{\rho} \right) \left(-\frac{\partial p}{\partial x} \right). \quad (10)$$

Where, ρ is the average density given by the equation $\rho = \alpha\rho_g + (1-\alpha)\rho_l$. The equation was derived by transforming equation (3), which is the momentum-conservation equation of the gas, into one-dimension.

The pressure-gradient term in equation (10) was written as

$$\frac{1}{p} \frac{dp}{dz} = \left(1 - \frac{1-\alpha}{\alpha} \right) \frac{M_e^2}{1-M_e^2} \frac{1}{A} \frac{dA}{dz}. \quad (11)$$

Where, M_e is the equilibrium Mach number and A is the cross-sectional area of the nozzle.

The divergence angle of the nozzle was set to 1.5 degrees, which was the same as that of the nozzle used in the experiment. The width of the inlet was defined as the characteristic length L , and the length of the diverging section of the nozzle was set as $4L$. The size of the back-pressure chamber after the nozzle was $10L \times 5L$.

Numerical calculation was made by applying the CIP method (Yabe *et al.*, 2004) in the basic equations. Unsteady two-dimensional calculation was carried out and the final solution was obtained when the pressure became constant.

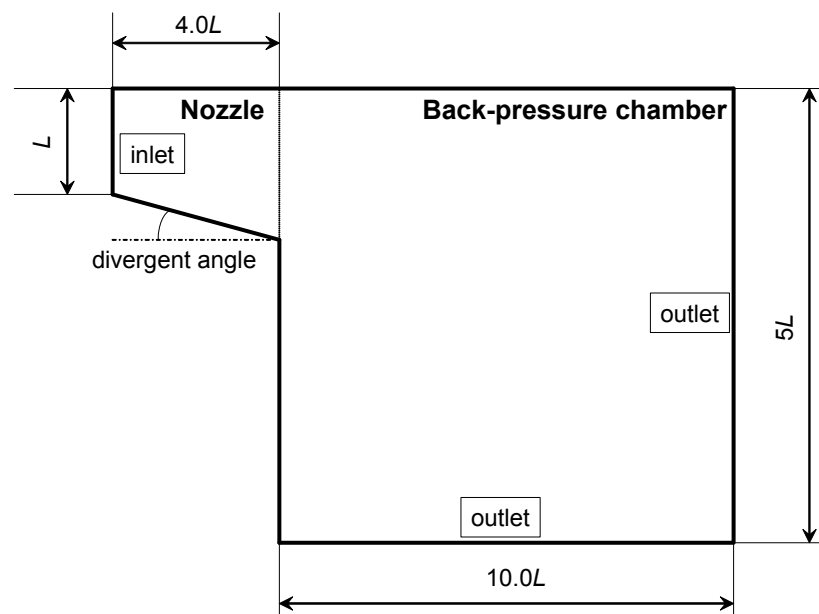


Figure 2: Flow field used in analytical model

5. RELATIONSHIP OF EXPANSION WAVES TO RELAXATION TIME

Figure 3 and Figure 4 show the streamline distribution for each phase calculated at different relaxation times. The given numerical parameters were inlet quality x_0 of 0.1, density ratio ρ_g/ρ_l of 1000 and non-dimensional inlet velocity u' of 0.5. There is a relative velocity between the vapor and the liquid throughout the nozzle. However,

steady state assumptions were applied to the nozzle inlet condition. Non-dimensional relaxation time was set to 0.1, and 1.0 in the simulation.

In the figures, dashed and solid lines show flow lines of the gas and the liquid, respectively. The sound speed, which governed the flow field, was the frozen sound speed and was almost equal to the sound speed of the gas. Although the inlet velocity was lower than this sound speed, the flow formed a supersonic flow field. When the relaxation time was short, the flow behaved as supersonic if the Mach number of the equilibrium sound speed was larger than unity even though the flow was subsonic based on the governing equations.

In the calculation, expansion waves did not occur when the inlet velocity was smaller than the equilibrium sound speed. Therefore, the simulated two-phase expansion waves showed supersonic characteristics even if the Mach number of the frozen sound speed was subsonic.

When the relaxation time became long, the liquid streamlines became much more straightened up compared to the gas streamlines. That was due to the increase in the inertial force of the droplets because the droplet size became larger when the relaxation time was increased.

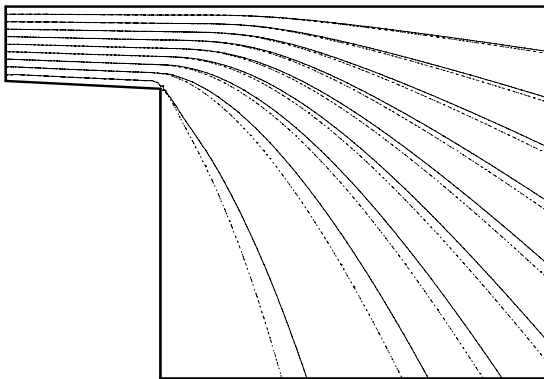


Figure 3: Expansion waves of two-phase flow at relaxation time $\tau' = 0.1$

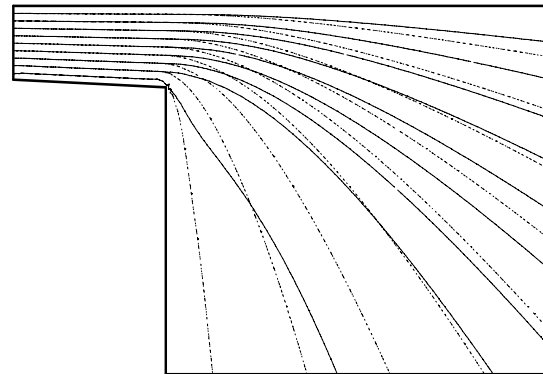


Figure 4: Expansion waves of two-phase flow at relaxation time $\tau' = 1.0$

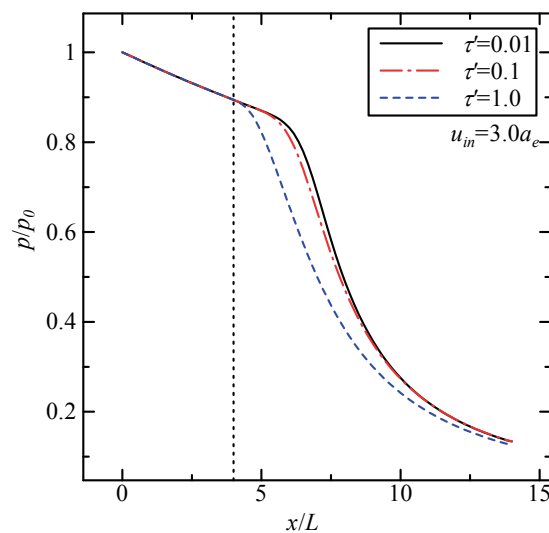


Figure 5: Pressure profiles along the channel center at several relaxation times

Figure 5 shows the pressure distributions along the centerline of the analytical area for relaxation times of 0.01, 0.1 and 1.0. The horizontal and the vertical axes were distance from the inlet of the analytical area and non-dimensional pressure, respectively. Inlet velocity, which was three times the equilibrium sound speed, and convergence angle of the nozzle equal to 1.5° were used in the analysis. The pressure distributions throughout the nozzle were the same for different relaxation times and they were almost linear. On the other hand, the pressure distributions after the nozzle became curves and they were different from each other because of their different relaxation times.

The axial locations where the expansion waves reached the centerline of the analytical area for the first time moved upstream although the inlet speed was the same. This trend of the expansion waves showed that the Mach number was decreasing with increasing relaxation time.

6. COMPARISON WITH THE EQUILIBRIUM THEORY

In gas dynamics, the semi-infinite flow which turns around an edge is known as the Prandtl-Meyer expansion fan. The pressure of the expansion wave in this case is shown as a function of the angle only. The relationship between the pressure and the expansion angle from the nozzle outlet was investigated in order to determine the expansion characteristics of two-phase flow.

An equation relating the expansion wave of equilibrium two-phase flow to the compressible characteristic of the vapor was derived. The assumptions used were that the pressure was proportional only to the density and that the velocities of the gas and the liquid were the same. When the velocity potential was expressed as $\varphi = r f(\theta)$, the expression

$$\left(\frac{df}{d\theta}\right)^2 = \left(\frac{dp}{d\rho}\right) \quad (12)$$

was obtained from the continuity and the momentum equations of two phase flow in the r - θ coordinate. Where, r is the coordinate in the radial direction from the edge of the nozzle outlet, and θ is the turn angle.

In case of potential flow, the mass-conservation equation of two-phase flow can be integrated. The integrated equation was written as

$$\frac{\partial}{\partial x_j} \left\{ \frac{v_j^2}{2} + \frac{p + K \log p}{K(\rho_{g0}/p_0) + \rho_l} \right\} = 0. \quad (13)$$

Where, the subscript 0 indicates inlet condition. The expression in the braces is conserved.

The following equation was obtained by combining the continuity equations (1) and (2) and the state equations (5) and (6).

$$v_j \frac{\partial}{\partial x_j} \left(\frac{\alpha p}{1 - \alpha} \right) = 0. \quad (14)$$

This equation was obtained because the expression in the parentheses was conserved along the flow line.

The term $\alpha p/(1-\alpha)$ in equation (14) was constant, so it was written as a constant K . Then, equation (12) was written as

$$\left(\frac{dp}{d\rho}\right) = \frac{(p + K)^2}{K\{K(\rho_{g0}/p_0) + \rho_l\}}. \quad (15)$$

Eventually, equation (13) became

$$\frac{f^2}{2} + \frac{(p + K)^2/(2K) + p + K \log p}{K \rho_{g0}/p_0 + \rho_l} = const. \quad (16)$$

In equation (16), p became a function of f only. Therefore equation (12) was resolved and the pressure was obtained as a function of the angle θ .

Figure 6 and Figure 7 show the pressure profiles obtained by using the Prandtl-Meyer equilibrium theory and those obtained by using the non-equilibrium theory. Inlet velocity, which was three times the equilibrium sound speed, and convergence angle of the nozzle equal to 1.5° were also used in this analysis. The selected values of non-dimensional relaxation times τ' were 0.1 and 10.0, respectively. The vertical axis is the non-dimensional pressure and the horizontal axis is the angle from the corner of the nozzle outlet.

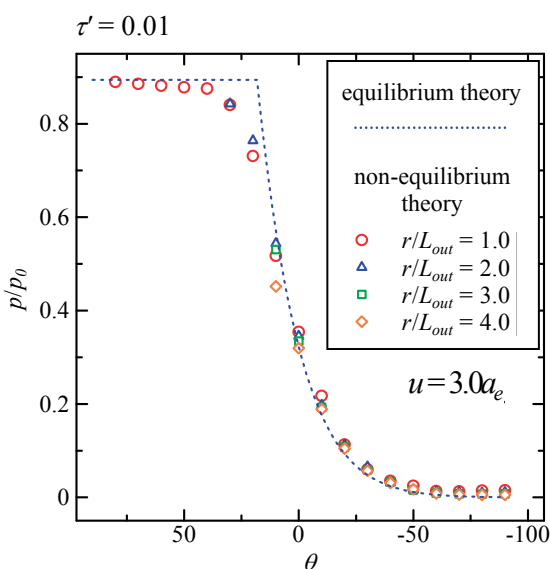


Figure 6: Pressure versus rotational angle for short relaxation time

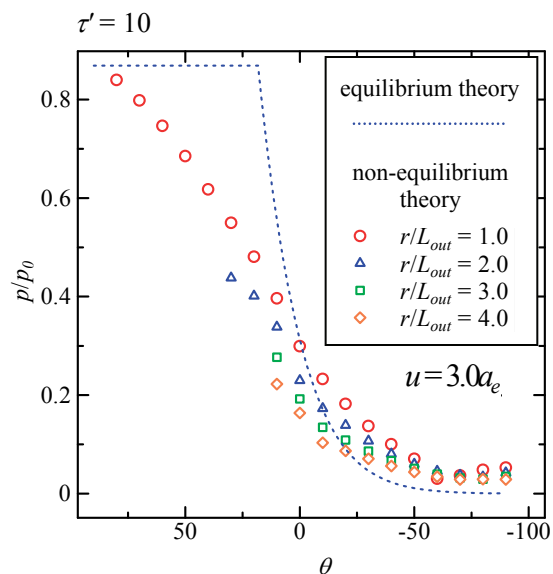


Figure 7: Pressure versus rotational angle for long relaxation time

When τ' was 0.01, the pressure profiles numerically simulated using the equilibrium theory and those using the non-equilibrium theory were almost the same. Therefore, the flow could be considered as equilibrium flow when non-dimensional relaxation time was smaller than 0.1. Oppositely, the numerical results using non-equilibrium theory did not agree well with those using the equilibrium theory when τ' was 10.0. In Figure 7, the pressure was decreasing with the increasing distance r/L_{out} from the edge. Then, the pressure profiles could not be expressed as a function of the angle θ only.

When the non-dimensional force was large, the frictional force between the gas and the liquid was also large because of the high velocity difference between the phases. Therefore, the attenuation of pressure could be attributed to the increase in the internal friction of two-phase flow.

7. COMPARISON WITH THE PREVIOUS EXPERIMENTAL RESULTS FOR STEAM

The steam expansion waves at nozzle outlet were previously investigated by us through experiment (Nakagawa *et al.*, 2007). As shown in Figure 8, the pressure distribution after the nozzle outlet, which was predicted by using the equilibrium theory, does not appear in the experimental pressure distribution. The results predicted by using the equilibrium theory do not match the experimental results because of non-equilibrium phenomena in two-phase flow.

The analytical result which considered non-equilibrium phenomena by momentum relaxation was plotted using solid curve in Figure 9. The non-dimensional relaxation time used in the analysis was 10. It was obtained from the physical properties of steam. The pressure profile from the analysis considering non-equilibrium momentum transfer does not have a flat upper part and is similar to the non-constant part of the experimental decompression curve. This pressure distribution shows that the start of expansion moves upstream because of the large pressure drop. The

pressure drop on the other hand is due to the energy loss created by the inter-phase momentum transfer at the outlet. Moreover, Mach number decreases near to unity due to the increasing sound speed of two-phase flow with momentum relaxation.

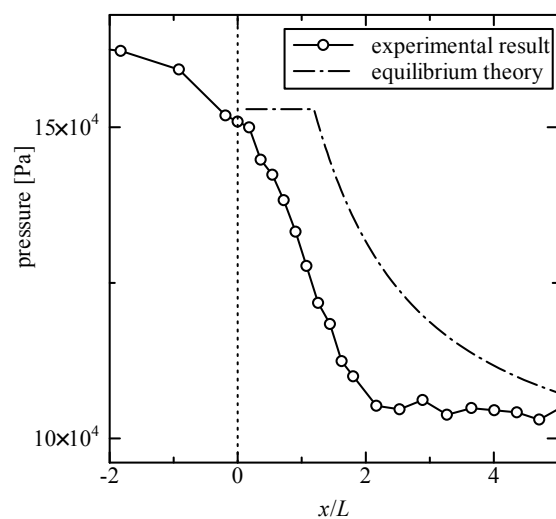


Figure 8: Experimental expansion curves along the center of the channel

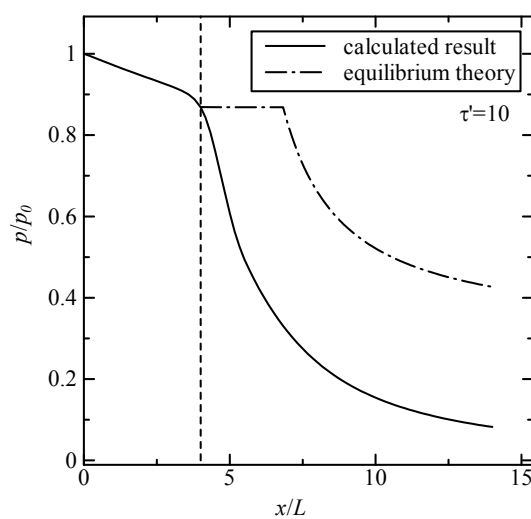


Figure 9: Calculated expansion curves along the center of the channel

8. CONCLUSION

The characteristics of the expansion wave in high-speed mist flow with velocity relaxation phenomenon were presented in this paper. It was shown that there were two types of sound speed in the high speed two-phase flow. One was the equilibrium sound speed and the other was the frozen sound speed. The sound speed was closer to the equilibrium sound speed when the relaxation time was short, but it was closer to the frozen sound speed when the relaxation time was long.

The start of expansion moved upstream with increasing relaxation time.

The pressure profiles simulated using non-equilibrium theory with relaxation phenomena resembled the pressure profiles from the experiments. Conversely, the pressure profiles simulated using the equilibrium theory were far from the pressure profiles obtained from the experiments. The non-equilibrium flow theory with relaxation phenomena could predict the behavior of expansion waves in supersonic two-phase flow more satisfactorily than the equilibrium flow theory.

REFERENCES

- Landau, L., Lifshitz, E., 1959, *Fluid Mechanics*, Pergamon Press., Oxford, 422 p.
- Marble, F., 1963, Dynamics of a Gas Containing Small Solid Particles, *Proc. 5th AGARD Combustion*: p. 175-215.
- Mori, Y., Suyama, J., 1980, *Geothermal Energy Reader*, Ohmsha, Ltd., Tokyo: p.168.
- Nakagawa, M., 2004, Refrigeration Cycle with Two-Phase Ejector, *Refrigeration*, vol. 79, no. 925: p.856-861.
- Nakagawa, M., Mamiya, N., 1986, Propagation of Rarefaction Waves in Bubble Flow with Evaporation, *Trans. of the JSME(B)*, vol.52, no.474: p. 650-656.
- Nakagawa, M., Miyazaki, H., Harada, A., Ibragimov, Z., 2007, Expansion Waves at the Outlet of the Supersonic Two-phase Flow Nozzle, *J. of Thermal Science and Technology*, vol.2, no.2: p. 291-300.
- Nakagawa, M., Takeuchi, H., Yokozeki, A., 1998, Performance of the Two-phase Nozzles Using the Refrigerant R134a, *Trans. of the JSME(B)*, vol. 64, no. 626: p. 3407-3413.
- Yabe, T., Mizoe, H., Takizawa, K., Moriki, H., Im, H., Ogata, Y., 2004, Higher-order Schemes with CIP Method and Adaptive Soroban Grid towards Mesh-free Scheme, *J. of Computational Physics*, vol. 194, no. 1: p.57-77.